

Article

Not peer-reviewed version

---

# Classifying the Role of Surface Ligands on the Passivation and Stability of $\text{Cs}_2\text{NaInCl}_6$ Double Perovskite Quantum Dots

---

Keita Tosa , Chao Ding <sup>\*</sup> , Shikai Chen , Shuzi Hayase , [Qing Shen](#) <sup>\*</sup>

Posted Date: 16 January 2024

doi: 10.20944/preprints202401.1178.v1

Keywords:  $\text{Cs}_2\text{NaInCl}_6$ ; quantum dots; stability; ligands; photoluminescence quantum yields



Preprints.org is a free multidiscipline platform providing preprint service that is dedicated to making early versions of research outputs permanently available and citable. Preprints posted at Preprints.org appear in Web of Science, Crossref, Google Scholar, Scilit, Europe PMC.

Copyright: This is an open access article distributed under the Creative Commons Attribution License which permits unrestricted use, distribution, and reproduction in any medium, provided the original work is properly cited.

Article

# Classifying the Role of Surface Ligands on the Passivation and Stability of Cs<sub>2</sub>NaInCl<sub>6</sub> Double Perovskite Quantum Dots

Keita Tosa <sup>1</sup>, Chao Ding <sup>2,\*</sup>, Shika Chen <sup>1</sup>, Shuzi Hayase <sup>1</sup> and Qing Shen <sup>1,\*</sup>

<sup>1</sup> Faculty of Informatics and Engineering, The University of Electro-Communications, 1-5-1 Chofugaoka, Chofu, Tokyo 182-8585, Japan

<sup>2</sup> Institute of New Energy and Low-Carbon Technology, Sichuan University, Chengdu 610065 China

\* Correspondence: shen@pc.uec.ac.jp (Q.S.); dc\_1107@foxmail.com (D.C.)

**Abstract:** Cs<sub>2</sub>NaInCl<sub>6</sub> double perovskites, which have excellent photoelectric conversion properties and are non-toxic and lead-free, have recently attracted much attention. In particular, double perovskite quantum dots (QDs) are considered to be a promising material for optoelectronic device applications. Ligands such as oleic acid (OA) and oleylamine (OAm) are essential for the synthesis of perovskite QDs, but their roles on double perovskite QDs are not yet clear. In this study, we have investigated the binding of OA and OAm to Cs<sub>2</sub>NaInCl<sub>6</sub> QDs through FTIR and NMR and their effects on the surface defect reduction and stability improvement for Cs<sub>2</sub>NaInCl<sub>6</sub> QDs. We found that only OAm was bound to the QD surfaces while OA was not. The OAm has a great effect on photoluminescence quantum yield (PLQY) improvement by passivate the QD surface defects. The stability of the QDs was also investigated, and it was shown that OA played a significant role in the stability of the QDs. Our findings provide critical insights into the roles of the ligands for photophysical properties and stability of lead free double perovskite QDs.

**Keywords:** Cs<sub>2</sub>NaInCl<sub>6</sub>; quantum dots; stability; ligands; oleylamine; oleic acid

## 1. Introduction

Lead halide perovskite with the molecular formula ABX<sub>3</sub> (A: CH<sub>3</sub>NH<sub>3</sub>, Cs etc., B: Pb, X: Cl, Br, I) have attracted much attention because of their remarkable optoelectronic properties and the potential applications such as solar cells, LED and light sources for displays [1–4]. Among these, quantum dots (QDs) have been the focus of much research in recent years due to their simplicity of synthesis and ease of application to devices [2,5–7]. However, the toxicity and instability of Pb-based perovskites greatly hinder the practical applications [8]. Thus, the study on Pb free perovskites is necessary and important.

Pb<sup>2+</sup> can be replaced by Sn<sup>2+</sup> or Ge<sup>2+</sup>, but Sn<sup>2+</sup> and Ge<sup>2+</sup> are unstable because they are easily oxidized to Sn<sup>4+</sup> and Ge<sup>4+</sup>, respectively [9,10]. Therefore, double perovskites with A<sub>2</sub>B'(I)B''(III)X<sub>6</sub>, in which Pb<sup>2+</sup> is replaced by monovalent and trivalent cations, have recently been studied [11,12]. Among them, Cs<sub>2</sub>NaInCl<sub>6</sub> with A: Cs<sup>+</sup>, B'(I): Na<sup>+</sup>, B''(III): In<sup>3+</sup>, and X: Cl has been studied as a promising material for solid-state lighting [13–17]. However, the low photoluminescence (PL) of this material is an issue due to its parity forbidden nature. Recently, Cs<sub>2</sub>NaInCl<sub>6</sub> doped with Sb<sup>3+</sup> broke the parity forbidden condition and went from a dark self-trapped excitons (STE) to a bright STE, resulting in a significant improvement in PL quantum yield (PLQY) of blue emission [14].

A major factor influencing the PLQY of Cs<sub>2</sub>NaInCl<sub>6</sub> double perovskite QDs is not only the Sb<sup>3+</sup> doping but also the surface ligands. In general, both oleic acid (OA) and oleylamine (OAm) are used to synthesize perovskite QDs, and these bind to the surface of the QDs and function as surface ligands, enabling the QDs to exist stably as a colloidal solution. Surface ligands are used to passivate the surface defect of the QDs and prevent them from coalescing with each other [18], and it is known that the stability can be improved by appropriately selecting them [19]. Much research has been

devoted to the binding of ligands to the QDs and the effects of ligands on the physical properties of QDs [20–23]. Elucidating the properties of the surface ligands is necessary to synthesize the QDs with high stability and high PLQY.

In this study, we investigate the effect of two kinds of ligands, i.e., OA and OAm on the optical properties and the stability of  $\text{Cs}_2\text{NaInCl}_6$  double perovskite QDs by adjusting the ratio of OA to OAm used during the QD synthesis. Fourier transform infrared spectroscopy (FTIR) and nuclear magnetic resonance (NMR) will be used to characterize the ligands states. The changes in various properties with the ratio of the two ligands are evaluated by measuring the PLQY, absorption and PL spectra, X-ray spectroscopy (XPS), X-ray diffraction patterns (XRD), and transmission electron microscopy (TEM) images. The roles of OAm and OA on the reduction of surface defects and improvement of the stability have been clarified.

## 2. Results and discussion

### 2.1. Synthesis of $\text{Cs}_2\text{NaInCl}_6$ QDs

$\text{Cs}_2\text{NaInCl}_6$  double perovskite QDs were synthesized by a modified method developed by Wang et al. [13].  $\text{Cs}(\text{OAc})$  (0.71 mmol),  $\text{Na}(\text{OAc})$  (0.5 mmol),  $\text{In}(\text{OAc})_3$  (0.495 mmol), and  $\text{Sb}(\text{OAc})_3$  (0.055 mmol) in octadecene (ODE) (9 mL) were placed in a three-neck flask. Then, OA and OAm were placed in a three-necked flask with different ratios, i.e.,  $[\text{OA}]/[\text{OAm}]$  is 4, 2, 1, 0.5 and 0.25, respectively, where  $[\text{OA}]+[\text{OAm}]=3.5$  mL. The mixture was heated to 110 °C and stirred under vacuum for 50 minutes, and then heated to 170 °C under nitrogen atmosphere, and a  $\text{GeCl}_4$  precursor solution containing 77  $\mu\text{L}$  of  $\text{GeCl}_4$  per 1 mL of ODE was swiftly injected. The solution was then heated to 180 °C. After 5 min, the reaction mixture was rapidly cooled in ice water to terminate the reaction. The reaction mixture was centrifuged at 9500 rpm for 5 min and the precipitate was collected. This precipitate was mixed with 10 mL of chlorobenzene, centrifuged at 9500 rpm for 5 min, and the precipitate was collected. The precipitate was thoroughly dried, dispersed in 4 mL of hexane, centrifuged at 4000 rpm for 5 min, and the supernatant containing the target quantum dots were collected.

### 2.2. Properties of $\text{Cs}_2\text{NaInCl}_6$ double perovskite QDs

The morphology and crystal structure of the synthesized QDs under the condition of  $[\text{OA}]/[\text{OAm}] = 4$  were characterized by TEM images and XRD pattern (Figure 1). The QDs showed a cubic shape. The average size of the QDs obtained from the TEM images was 11.2 nm, and the size estimated from the XRD diffraction pattern was 11.6 nm using Scherrer equation. The XRD pattern is consistent with the that of  $\text{Cs}_2\text{NaInCl}_6$  [14], indicating  $\text{Cs}_2\text{NaInCl}_6$  QDs have been synthesized successfully.

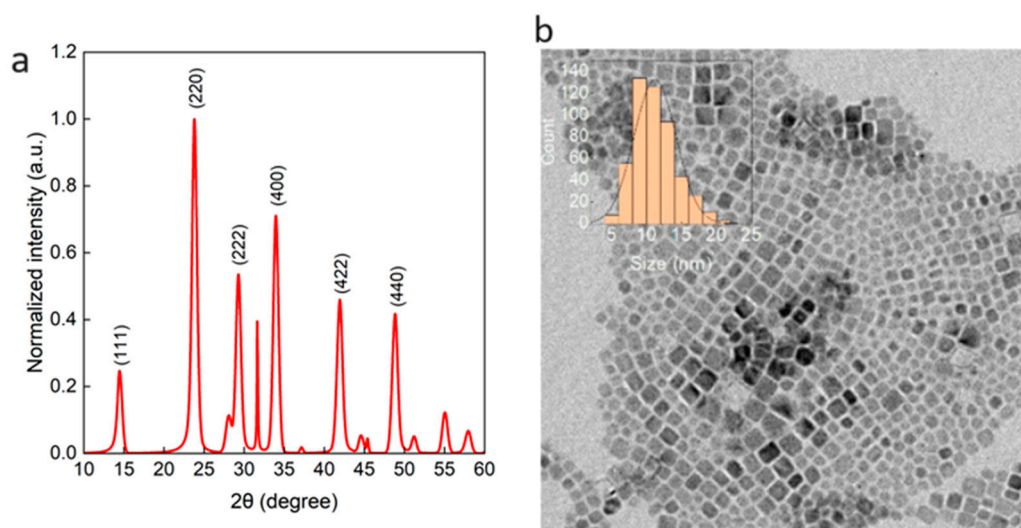


**Figure 1.** (a) XRD pattern and (b) TEM image of cfc synthesized with the condition of  $[OA]/[OAm]=4$ .

Figure 2 shows typical PL, optical absorption and PL excitation (PLE) spectra of the synthesized QDs under the condition of  $[OA]/[OAm] = 4$ , respectively. From the PL spectrum, a blue emission with a peak wavelength of 450 nm can be observed clearly. The PLQY of this luminescence was about 85%. In Figure 2(b), besides the optical absorption spectrum (top), its second derivative spectrum (bottom) is also shown. The second-order differentiation of the absorption spectrum can be very useful for analyzing the spectrum of which the peaks are difficult to see, because it is known that the minima of the second derivative spectrum correspond to the peaks in the optical absorption spectrum [24]. Therefore, two absorption peaks at 320 nm and 335 nm can be observed clearly. These peaks are obtained by doping antimony (Sb), and when combined with the PLE (Figure 2 (c)) peaks, the emission is strong at these absorption peaks. This broad blue luminescence has been reported to originate from the STE in the  $Cs_2NaInCl_6$  QDs [14].

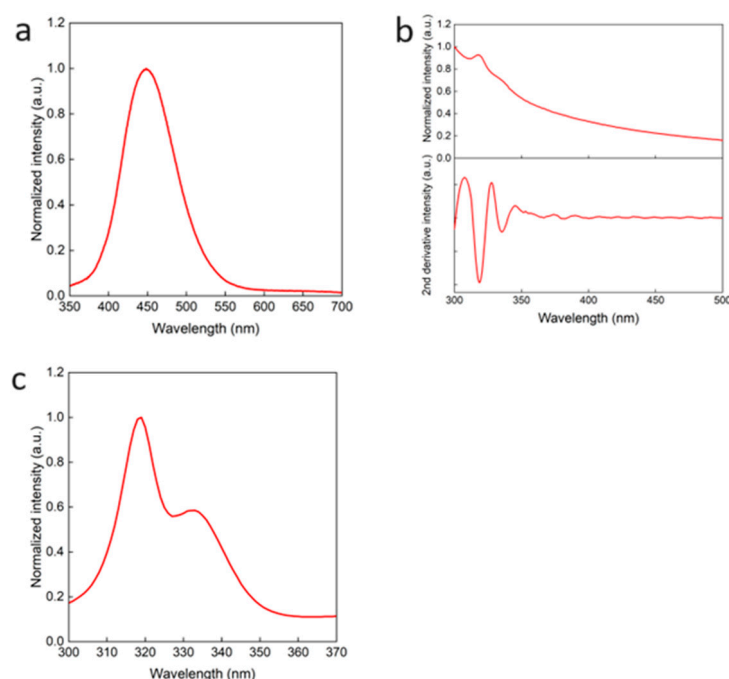


**Figure 2.** (a) PL spectrum obtained with excitation wavelength of 320 nm, (b) optical absorption spectrum (top) and its second derivative spectrum (bottom), and (c) PL excitation (PLE) spectrum of  $Cs_2NaInCl_6$  QDs synthesized with the condition of  $[OA]/[OAm]=4$ .

### 2.3. OA and OAm states in $Cs_2NaInCl_6$ double perovskite QDs

OA and OAm are used in the synthesis of the QDs, which are expected to bind to the QDs produced. To confirm this expectation, FTIR and NMR measurements were carried out. Figure 3 shows the FTIR spectra of four kinds samples:  $Cs_2NaInCl_6$  QDs, OAm, OA and mixture of OAm and OA. The characteristic peak of OA was obtained at  $1710\text{ cm}^{-1}$ . This peak is also observed in the QD solution. The broad peaks at  $1640\text{ cm}^{-1}$  and  $1555\text{ cm}^{-1}$  are thought to be the peaks of deprotonated OA and protonated OAm, which are also partly contained in the QD solution. Finally, the peak at  $1585\text{ cm}^{-1}$ , which is only observed in the QD solution, is considered to be a shifted peak of ionized OA or ionized OAm. These results indicate that the QD solution contains OA, deprotonated OA, and protonated OAm.

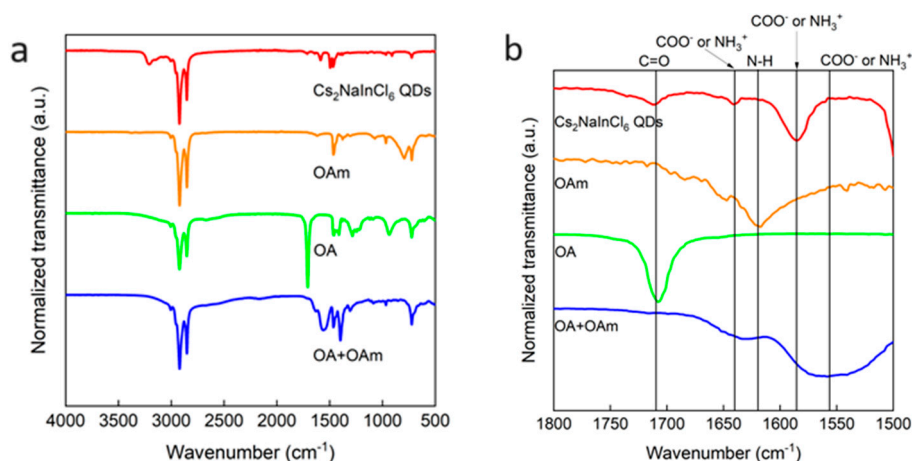


**Figure 3.** (a) FTIR spectra of  $\text{Cs}_2\text{NaInCl}_6$  QDs synthesized with  $[\text{OA}]/[\text{OAm}]=4$ , OAm, OA and mixture of OAm and OA. (b) Enlarged region of (a) where characteristic peaks for OA and OAm can be observed clearly.

However, it is impossible to determine whether the two kinds of ligands are bound to the QDs or not only by the FTIR results. Therefore, NMR measurements were performed. Figure 4(a) shows the results of  $^1\text{H}$ NMR. In the QDs solution, the 3 and 6 protons common to OA and OAm, as well as the 1 and 2 peaks characteristic of OA, were observed. The sharp peak seen around 2.17 ppm was acetone used to clean the sample tube [25]. The amine peak of OAm could not be observed because the amount of OAm in the solution was small or because it was close to the surface [26]. Therefore, we dropped 10  $\mu\text{L}$  of OA and OAm into the QD solution and measured them (Figure 4(b)). In the sample with OA, the OA peak at 2.33 ppm was enhanced, but the peak did not shift, and no broadening of the peak was observed. This indicates that there is no interaction between OA ligand and the QDs, which suggest that OA is not bound to the QDs. On the other hand, the  $\beta$  peak at 2.66 ppm was shifted in the sample with the addition of OAm. This is because the OAm binding to the QDs restricts the longitudinal relaxation, resulting in a broadening of the peak due to the predominance of transverse relaxation [27,28]. These results indicate that there is an interaction between OAm ligand and the QDs.

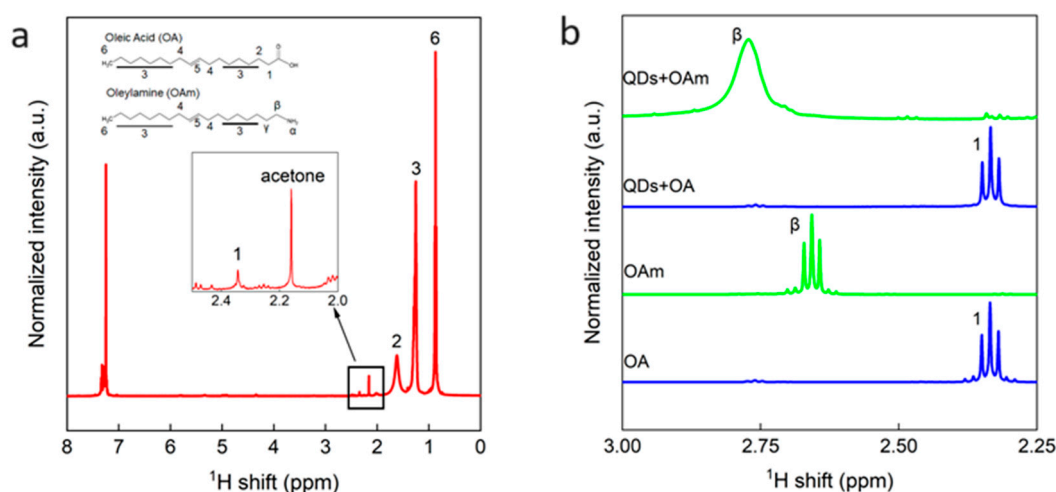


**Figure 4.** (a) NMR spectrum of  $\text{Cs}_2\text{NaInCl}_6$  QDs synthesized with the condition of  $[\text{OA}]/[\text{OAm}]=4$ . (b) NMR spectrum with enlarged region where characteristic peaks for OA and OAm can be observed clearly. Measurements were made for QDs solutions with addition of 10  $\mu\text{L}$  of OA and OAm, respectively, and pure OA and OAm.

Nuclear Overhauser Spectroscopy (NOESY) was further performed to provide evidence that OA is not bound to the QDs but OAm is bound (Figure 5). First, nothing could be measured when only the QD solution was used. This is thought to be due to the same reason as for  $^1\text{H}$ NMR. Next, we measured the QD solution with OA or OAm added, as in  $^1\text{H}$ NMR measurements. Red contour lines were observed in the sample with OA addition. This is a positive NOE signal, which is evidence that the QDs are not bound with OA. Next, a negative NOE signal was observed in the sample to which OAm was added. This is the evidence that the OAm is bound to the QDs. This is thought to be because the unbound ligand behaves as a small molecule, while the bound ligand behaves as a large molecule [29].

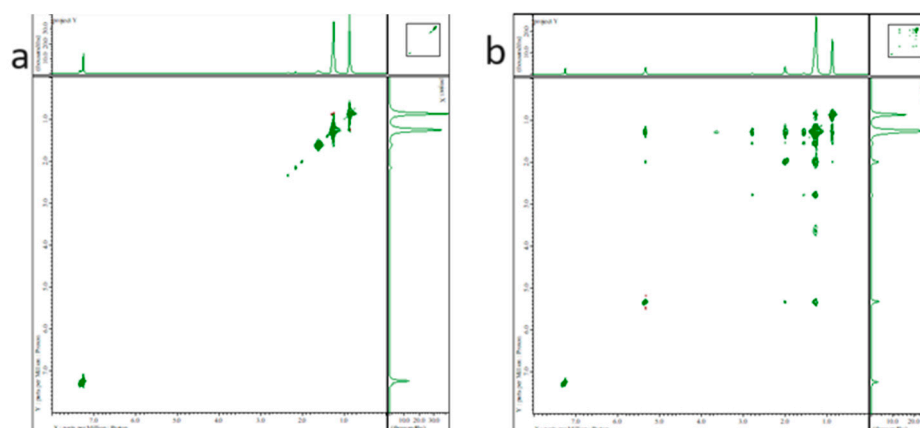
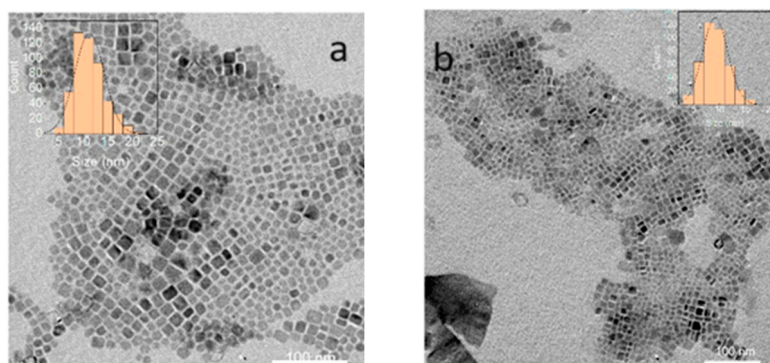


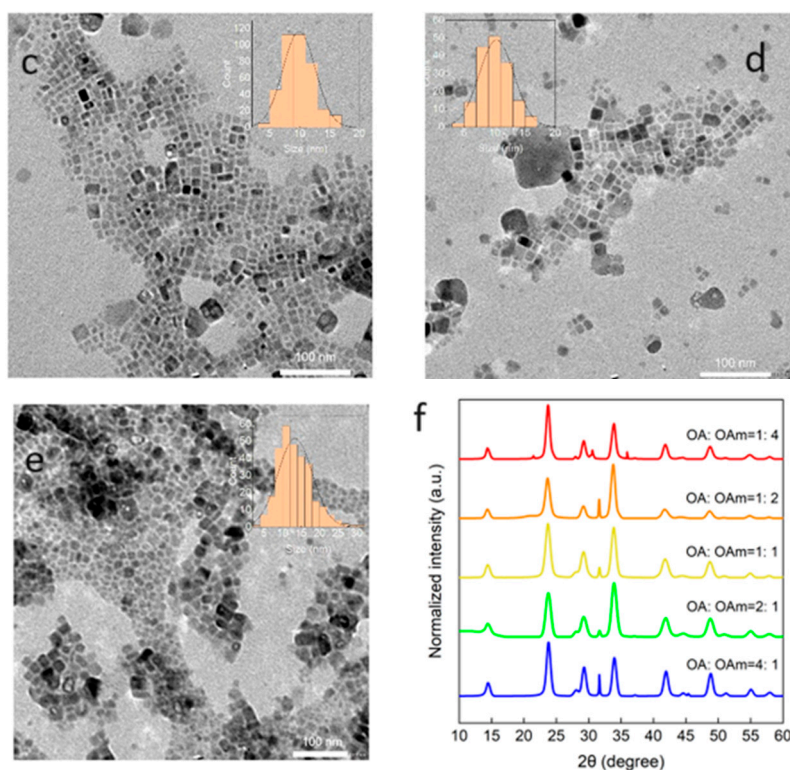
**Figure 5.** NOESY spectra of  $\text{Cs}_2\text{NaInCl}_6$  QDs synthesized with the condition of  $[\text{OA}]/[\text{OAm}]=4$ , in which 10  $\mu\text{L}$  of OA was added (a) or 10  $\mu\text{L}$  of OAm was added (b).

#### 2.4. Roles of OA and OAm on $\text{Cs}_2\text{NaInCl}_6$ QDs

Based on the above results, it was shown that only OAm is bound to the QDs. Next, it is important and necessary to elucidate the respective roles of OA and OAm on the photophysical properties such PLQY and the stability. Therefore, we prepared five kinds of QDs by changing the ratio of [OA] and [OAm] in the synthesis process, i.e.,  $[\text{OA}]/[\text{OAm}]$  is 4, 2, 1, 0.5, and 0.25, respectively.

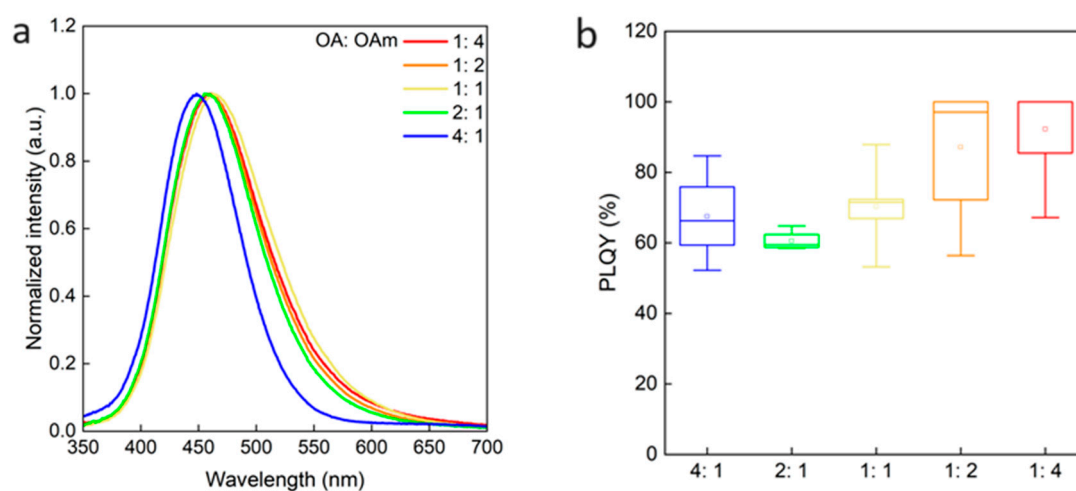
The TEM images and the XRD pattern of the five kinds of QDs shown in Figure 6. In a previous study, it was reported that the shape of the QDs changed when synthesized by changing the ratio of OA and OAm [30]. However, the synthesized QDs here generally show cubic shapes (Figure 6(a)-(e)). In addition, XRD results showed that the crystal structure of the QDs are cubic for all kinds of samples (Figure 6(f)), and the average sizes of the QDs obtained from the TEM images were 11.2, 9.2, 9.9, 10.3, and 13.4 nm when  $[\text{OA}]/[\text{OAm}]$  was 4, 2, 1, 0.5, and 0.25, respectively.





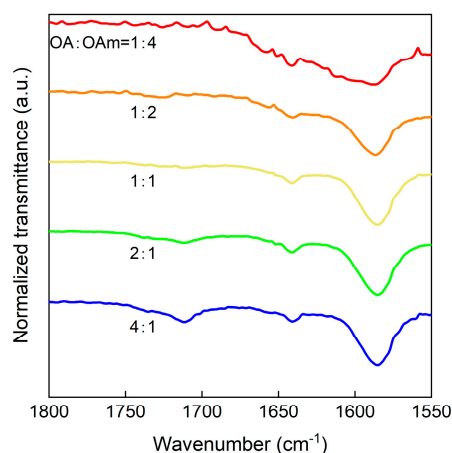
**Figure 6.** TEM images of  $\text{Cs}_2\text{NaInCl}_6$  QDs synthesized with (a)  $[\text{OA}]/[\text{OAm}]=4$ , (b)  $[\text{OA}]/[\text{OAm}]=2$ , (c)  $[\text{OA}]/[\text{OAm}]=1$ , (d)  $[\text{OA}]/[\text{OAm}]=0.5$ , and (e)  $[\text{OA}]/[\text{OAm}]=0.25$ , respectively. (f) XRD patterns of the five kinds of QDs synthesis with different  $[\text{OA}]/[\text{OAm}]$ .

Figure 7(a) and (b) show the PL spectra and PLQY of the five kinds of QDs, respectively. As the  $[\text{OA}]/[\text{OAm}]$  changed, the PL peak wavelength was almost the same and the shift of a few nm is maybe due to a little concentration change of the QD solution. On the other hand, the PLQY increased as  $[\text{OA}]/[\text{OAm}]$  was decreased, i.e., as the ratio of OAm increased as shown in Figure 7(b). In addition, the PLQY could be achieved close to 100% when  $[\text{OA}]/[\text{OAm}]$  was 0.5 and 0.25, respectively. The high PLQY is thought to be due to the passivation of surface defects of the QDs when the OAm ratio was increased in the synthesis. From the previous result that only OAm was bound to the QDs, it is clear that it is OAm ligand has the role to passivate the surface defects of the  $\text{Cs}_2\text{NaInCl}_6$  QDs.



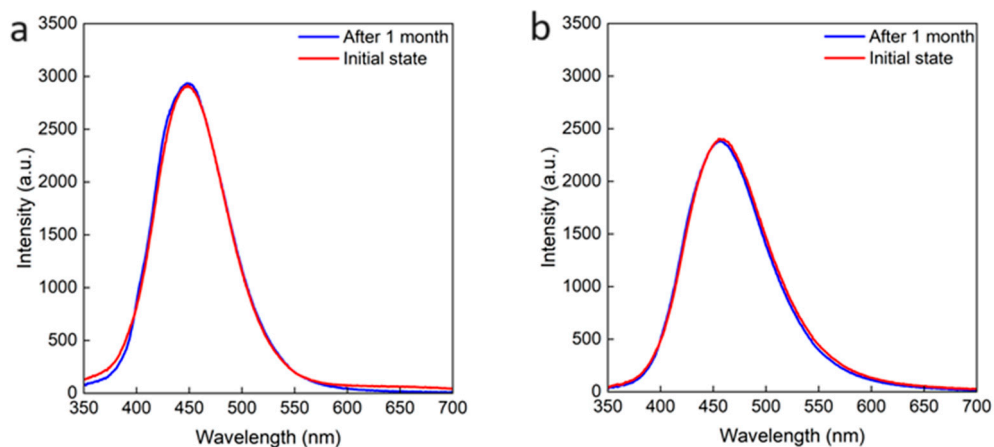
**Figure 7.** (a) PL spectra and (b) PLQY of  $\text{Cs}_2\text{NaInCl}_6$  QDs synthesized with different  $[\text{OA}]/[\text{OAm}]$ .

FTIR measurement was performed to investigate the OA and OAm in the QD solution for different  $[OA]/[OAm]$  (Figure 8). As a result, the C=O peak at  $1710\text{ cm}^{-1}$ , which is a characteristic of OA, became smaller as  $[OA]/[OAm]$  decreased, and no peak was observed when  $[OA]/[OAm]$  was 0.5 and 0.25. This indicates that there is little residual OA in the QD solution.



**Figure 8.** FTIR spectra of  $\text{Cs}_2\text{NaInCl}_6$  quantum dots synthesized by changing  $[OA]/[OAm]$ .

Next, to investigate the change in stability when the  $[OA]/[OAm]$  changes, we measured and compared the PL spectra of the five kinds of samples after one month of storage at room temperature and in air. For the samples with  $[OA]/[OAm]$  of 4, 2, and 1, the PL spectra and the PL intensity were not changed after one month, indicating that the QDs were not degraded. On the other hand, for  $[OA]/[OAm]$  of 0.5 and 0.25, the PL intensity decreased and the PL spectrum also changed after one month, indicating that the stability of the QDs became worse when the OA ratio was decreased. In summary, the samples with high OA content showed high stability. This is thought to be because OA can ionize OAm, the latter are then reattached to the QDs after they leaved the QDs. In samples where the QD solution did not contain enough OA, it is thought that the OA could not reionize the released OAm.



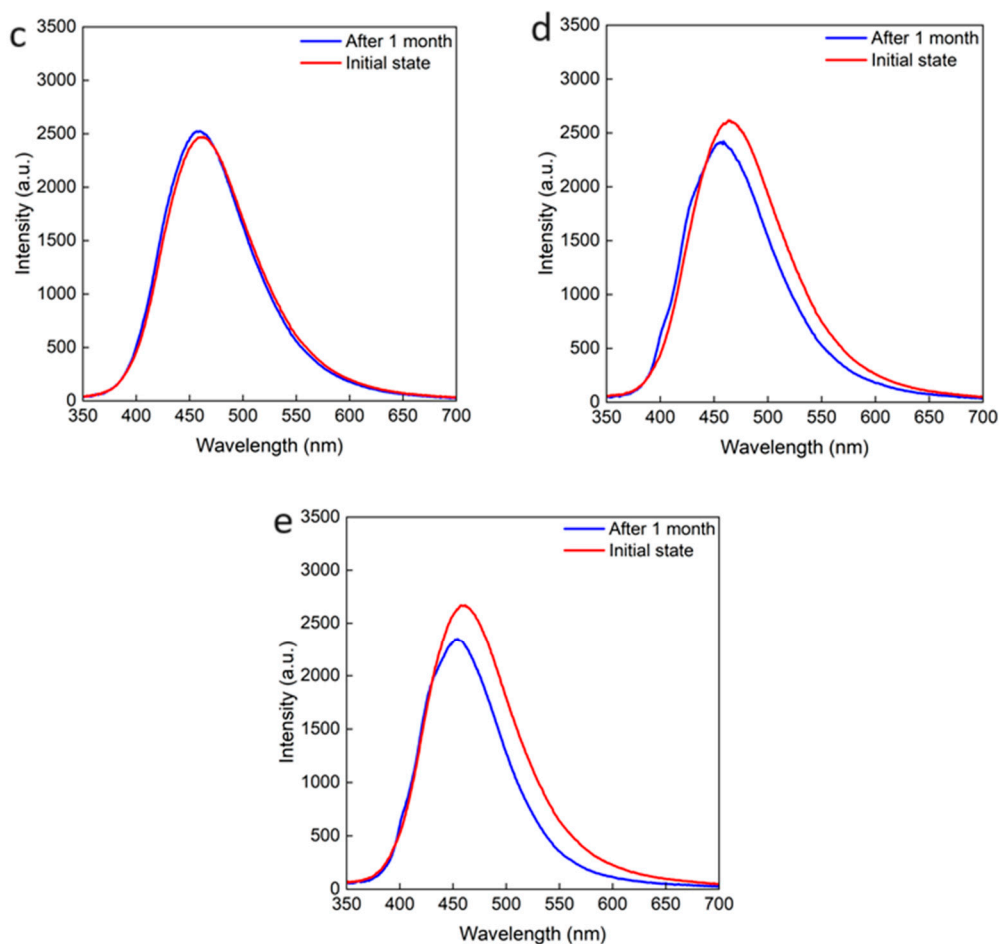


**Figure 9.** PL spectra of  $\text{Cs}_2\text{NaInCl}_6$  QDs synthesized at (a)  $[\text{OA}]/[\text{OAm}]=4$ , (b)  $[\text{OA}]/[\text{OAm}]=2$ , (c)  $[\text{OA}]/[\text{OAm}]=1$ , (d)  $[\text{OA}]/[\text{OAm}]=0.5$  and (e)  $[\text{OA}]/[\text{OAm}]=0.25$ , respectively, which were measured soon after preparation and stored at room temperature and in air for 1 month.

To confirm that OA ionizes OAm and binds it back to the QDs, we compared the stability of a sample of QD solution with  $[\text{OA}]/[\text{OAm}]$  of 0.25 and a sample added with OAm when stored at room temperature and in air for 72 hours (Figure 10). The QDs precipitated in the pure QD and OAm-added samples. On the other hand, no precipitation was observed in the sample to which oleic acid was added. This indicates that OA ionizes OAm and binds it to the QDs, as expected above.



**Figure 10.** Stability of the QD solutions prepared with  $[\text{OA}]/[\text{OAm}]=0.25$ . From left to right: QDs solution; QD solution with OAm; QD solution with OA.

### 3. Conclusions

To elucidate the states of OA and OAm ligands in the Cs<sub>2</sub>NaInCl<sub>6</sub> QDs solution synthesized with [OA]/[OAm]=4, FTIR and NMR measurements were performed. The FTIR measurements revealed the presence of OA, deprotonated OA and protonated OAm in the QD solution. Next, NMR measurements showed that OA and the QDs do not interact and are not bound to each other. On the other hand, OAm and QDs interacted with each other, indicating that they are bound. The results of synthesizing the QDs with different OA/OAm ratios showed that OAm contributes to the PLQY enhancement by passivate the surface defects of the QDs. On the other hand, OA was found to contribute to high stability by protonating OAm. Our findings offer critical insights into the roles of OA and OAm for photophysical properties and stability of lead free double perovskite QDs and lays a foundation for future research and technological advancements in this domain.

**Funding:** This research was supported by the Japan Science and Technology Agency (JST) Mirai program (JPMJMI17EA), MEXT KAKENHI Grant (26286013, 17H02736).

**Data Availability Statement:** The data that support the findings of this study are available from the corresponding author upon reasonable request.

**Conflicts of Interest:** The authors declare no conflict of interest.

### References

1. T. Chiba, Y. Hayashi, H. Ebe, K. Hoshi, J. Sato, S. Sato, Y. Jin Pu, S. Ohisa, and J. Kido, "Anion-exchange red perovskite quantum dots with ammonium iodine salts for highly efficient light-emitting devices", *Nature Photon*, 12, 681 (2018).
2. A. Swaenker, A. Marshall, E. Sanehira, B. Chernomordik, D. Moore, J. Christinas, T. Chakrabarti, and J. Luther, "Quantum dot-induced phase stabilization of a-CsPbI<sub>3</sub> perovskite for high-efficiency photovoltaics", *Science*, 354, 92 (2016).
3. X. Li, F. Cao, D. Yu, J. Chen, Z. Sun, Y. Shen, Y. Zhu, L. Wang, Y. Wei, Y. Wu, H. Zeng, "All Inorganic Halide Perovskites Nanosystem: Synthesis, Structural Features, Optical Properties and Optoelectronic Applications", 13, 1603996 (2017).
4. M. Green, A. Ho-Baillie, and H. Snaith, "The emergence of perovskite solar cells", *Nature Photon*, 8, 506 (2014).
5. L. Protesescu, S. Yakunin, M. Bodnarchuk, F. Krieg, R. Caputo, C. Hendon, R. Yang, A. Walsh, and M. Kovalenko, "Nanocrystals of Cesium Lead Halide Perovskites (CsPbX<sub>3</sub>, X = Cl, Br, and I): Novel Optoelectronic Materials Showing Bright Emission with Wide Color Gamut", *Nano Lett.*, 15, 3692 (2015).
6. X. Du, G. Wu, J. Chenga, H. Danga, K. Maa, Y. Zhanga, P. Tana, and S. Chen, "High-quality CsPbBr<sub>3</sub> perovskite nanocrystals for quantum dot light-emitting diodes", *RSC Adv.*, 7, 10391 (2017).
7. H. Utzat, W. Sun, A. Kaplan, F. Krieg, M. Ginterseder, B. Spokoyny, N. Klein, K. Shulenberger, C. Perkinson, M. Kovalenko, and M. Bawendi, "Coherent single-photon emission from colloidal lead halide perovskite quantum dots", *Science*, 363, 1068 (2019).
8. H. Huang, M. Bodnarchuk, S. Kershaw, M. Kovalenko, and A. Rogach, "Lead Halide Perovskite Nanocrystals in the Research Spotlight: Stability and Defect Tolerance", *ACS Energy Lett.*, 2, 2071 (2017).
9. N. Noel, S. Stranks, A. Abate, C. Wehrenfennig, S. Guarnera, A. Haghighirad, A. Sadhanala, G. Eperon, S. Pathak, M. Johnston, A. Petrozza, L. Herza, and H. Snaith, "Lead-free organic-inorganic tin halide perovskites for photovoltaic applications", *Energy Environ. Sci.*, 7, 3061 (2014).
10. I. Kopacic, B. Friesenbichler, S. Hoefler, B. Kunert, H. Plank, T. Rath, and G. Trimmel, "Enhanced Performance of Germanium Halide Perovskite Solar Cells through Compositional Engineering", *ACS Appl. Energy Mater.*, 1, 343 (2018).
11. Y. Liu, A. Nag, L. Manna, and Z. Xia, "Lead-Free Double Perovskite Cs<sub>2</sub>AgInCl<sub>6</sub>", *Angew. Chem. Int. Ed.*, 60, 11592 (2021).
12. J. Zhou, X. Rong, P. Zhang, M. Molokeev, P. Wei, Q. Liu, X. Zhang, Z. Xia, "Manipulation of Bi<sup>3+</sup>/In<sup>3+</sup> Transmutation and Mn<sup>2+</sup>-Doping Effect on the Structure and Optical Properties of Double Perovskite Cs<sub>2</sub>NaBi<sub>1-x</sub>In<sub>x</sub>Cl<sub>6</sub>", *Adv. Opt. Mater.*, 7, 1801435 (2019).
13. X. Wang, T. Bai, B. Yang, R. Zhang, D. Zheng, J. Jiang, S. Tao, F. Liu, and K. Han, "Germanium Halides Serving as Ideal Precursors: Designing a More Effective and Less Toxic Route to High-Optoelectronic-Quality Metal Halide Perovskite Nanocrystals", *Nano Lett.*, 22, 636 (2022).
14. R. Zeng, L. Zhang, Y. Xue, B. Ke, Z. Zhao, D. Huang, Q. Wei, W. Zhou, and B. Zou, "Highly Efficient Blue Emission from Self-Trapped Excitons in Stable Sb<sup>3+</sup>-Doped Cs<sub>2</sub>NaInCl<sub>6</sub> Double Perovskites", *J. Phys. Chem. Lett.*, 11, 2053 (2020).

15. B. Zhou, Z. Liu, S. Fang, H. Zhong, B. Tian, Y. Wang, H. Li, H. Hu, and Y. Shi, "Efficient White Photoluminescence from Self-Trapped Excitons in Sb<sup>3+</sup>/Bi<sup>3+</sup>-Codoped Cs<sub>2</sub>NaInCl<sub>6</sub> Double Perovskites with Tunable Dual-Emission", *ACS Energy Lett.*, 6, 3343 (2021).
16. X. Liu, X. Xu, B. Li, L. Yang, Q. Li, H. Jiang, and D. Xu, "Tunable Dual-Emission in Monodispersed Sb<sup>3+</sup>/Mn<sup>2+</sup> Codoped Cs<sub>2</sub>NaInCl<sub>6</sub> Perovskite Nanocrystals through an Energy Transfer Process", *Small*, 16, 2002547 (2020).
17. R. Ahmad, L. Zdražil, S. Kalytchuk, A. Naldoni, A. Rogach, P. Schmuki, R. Zboril, and S. Kment, "Uncovering the Role of Trioctylphosphine on Colloidal and Emission Stability of Sb-Alloyed Cs<sub>2</sub>NaInCl<sub>6</sub> Double Perovskite Nanocrystals", *ACS Appl. Mater. Interfaces*, 13, 47845 (2021).
18. F. Remacle, and R. Levine, "Quantum Dots as Chemical Building Blocks: Elementary Theoretical Considerations", *Chemphyschem*, 2, 20 (2001).
19. Y. Chen, S. Smock, A. Flintgruber, F. Perras, R. Brutchey, and A. Rossini, "Surface Termination of CsPbBr<sub>3</sub> Perovskite Quantum Dots Determined by Solid-State NMR Spectroscopy", *J. Am. Chem. Soc.*, 142, 6117 (2020).
20. M. Boles, D. Ling, T. Hyeon, and D. Talapin, "The surface science of nanocrystals", *Nature Mater*, 15, 141 (2016).
21. J. Roo, M. Ibáñez, P. Geiregat, G. Nedelcu, W. Walravens, J. Maes, J. Martins, I. Driessche, M. Kovalenko, and Z. Hens, "Highly Dynamic Ligand Binding and Light Absorption Coefficient of Cesium Lead Bromide Perovskite Nanocrystals", *ACS Nano*, 10, 2071 (2016).
22. Z. Hens, and J. Martins, "A Solution NMR Toolbox for Characterizing the Surface Chemistry of Colloidal Nanocrystals", *Chem. Mater.*, 25, 1211 (2013).
23. V. Ravi, P. Santra, N. Joshi, J. Chugh, S. Singh, H. Rensmo, P. Ghosh, and A. Nag, "Origin of the Substitution Mechanism for the Binding of Organic Ligands on the Surface of CsPbBr<sub>3</sub> Perovskite Nanocubes", *J. Phys. Chem. Lett.*, 8, 4988 (2017).
24. A. Owen, "Uses of Derivative Spectroscopy", Agilent Technologies (1995).
25. G. Fulmer, A. Miller, N. Sherden, H. Gottlieb, A. Nudelman, B. Stoltz, J. Bercaw, and K. Goldberg, "NMR Chemical Shifts of Trace Impurities: Common Laboratory Solvents, Organics, and Gases in Deuterated Solvents Relevant to the Organometallic Chemist", *Organometallics*, 29, 2179 (2010).
26. J. Roo, Y. Justo, K. Keukeleere, F. Broeck, J. Martins, I. Driessche, and Z. Hens, "Carboxylic-Acid-Passivated Metal Oxide Nanocrystals: Ligand Exchange Characteristics of a New Binding Motif", *Angew. Chem. Int. Ed.*, 54, 6488 (2015).
27. J. Sachleben, E. Wooten, L. Emsley, A. Pines, V. Colvin, and P. Alivisatos, "NMR studies of the surface structure and dynamics of semiconductor nanocrystals", *Chem. Phys. Lett.*, 198, 431 (1992).
28. M. Hostetler, J. Wingate, C. Zhong, J. Harris, R. Vachet, M. Clark, J. Londono, S. Green, J. Stokes, G. Wignall, G. Glish, M. Porter, N. Evans, and R. Murray, "Alkanethiolate Gold Cluster Molecules with Core Diameters from 1.5 to 5.2 nm: Core and Monolayer Properties as a Function of Core Size", *Langmuir*, 14, 17 (1998).
29. B. Fritzing, I. Moreels, P. Lommens, R. Koole, Z. Hens, and J. Martins, "In Situ Observation of Rapid Ligand Exchange in Colloidal Nanocrystal Suspensions Using Transfer NOE Nuclear Magnetic Resonance Spectroscopy", *J. Am. Chem. Soc.*, 131, 3024 (2009).
30. Y. Zhang, T. Shah, F. Deepak, and B. Korgel, "Surface Science and Colloidal Stability of Double-Perovskite Cs<sub>2</sub>AgBiBr<sub>6</sub> Nanocrystals and Their Superlattices", *Chem. Mater.*, 31, 7962 (2019).

**Disclaimer/Publisher's Note:** The statements, opinions and data contained in all publications are solely those of the individual author(s) and contributor(s) and not of MDPI and/or the editor(s). MDPI and/or the editor(s) disclaim responsibility for any injury to people or property resulting from any ideas, methods, instructions or products referred to in the content.